Vol. 50 (2019) *Acta Physica Polonica B* No 7

CLUSTER DECAY HALF-LIFE WITH DOUBLE-FOLDING POTENTIAL: UNCERTAINTY ANALYSIS

N. Maroufi, V. Dehghani[†], S.A. Alavi

Department of Physics, University of Sistan and Baluchestan, Zahedan, Iran

(Received September 29, 2018; accepted April 30, 2019)

Cluster decay half-lives of some cluster emitters were calculated by using microscopic potential in framework of semiclassical WKB method with considering the Bohr–Sommerfeld quantization. The microscopic double-folding potential was used for cluster–daughter nuclear potential. By considering the uncertainty of the radius and surface diffuseness in double-folding nuclear potential, the uncertainties of the cluster decay half-lives have been determined. The calculated half-lives with double-folding potential were in reasonable agreement with experimental data.

DOI:10.5506/APhysPolB.50.1349

1. Introduction

Cluster radioactivity is somewhat recent topic in nuclear physics, and several theoretical studies [1–4] and experiments [5–9] have been performed after first prediction in 1980 [10] and first foundation in 1984 [11]. From theoretical point of view, the cluster decay half-life can be determined from semiclassical WKB method, in which effective potential between cluster–daughter system plays a crucial role in calculations. The nuclear potential as an important part of the effective potential may significantly change the results. So, its proper selection is imperative. Different microscopic [12–14] and phenomenological macroscopic [15–20] nuclear potentials have been introduced and adopted in literature for nuclear potential. For instance, in Ref. [14], the cluster decay process has been investigated by using density-dependent double-folding potential. In Refs. [16, 17], the Woods–Saxon, squared Woods–Saxon, and Cosh potentials have been used for nuclear potential. By means of fourteen proximity potentials, the cluster decay half-lives of even–even cluster emitters have been calculated in Ref. [18].

[†] Corresponding author: vdehghani@phys.usb.ac.ir

Our aim in this study is to calculate the cluster decay half-lives of some cluster emitters with heavy clusters by using double-folding potential, Woods–Saxon potential, and cut-off Woods–Saxon potential. In Sec. 2, the theoretical model is introduced. The obtained results and discussion are given in Sec. 3. Finally, the concluding remarks are given in Sec. 4.

2. Theoretical method

The cluster decay half-life, $T_{1/2}$, can be calculated by means of semiclassical WKB approximation as

$$T_{1/2} = \frac{\ln 2}{\lambda}\,, \tag{1}$$

where λ is the decay constant given as

$$\lambda = \nu P S_{\mathrm{c}}\,, \tag{2}$$

where ν, P, S_{c} are assault frequency, tunneling probability, and cluster preformation probability, respectively. The assault frequency is obtained as [22]

$$\nu = \frac{\hbar}{2\mu}\left[\int\limits_{r_1}^{r_2} \frac{\mathrm{d}r}{\sqrt{\frac{2\mu}{\hbar^2}|Q - V(r)|}}\right]^{-1}. \tag{3}$$

The tunneling probability of cluster nucleus through barrier in subbarrier energies is given as

$$P = \frac{1}{1+e^q}\,, \tag{4}$$

$$q = \frac{2\sqrt{2\mu}}{\hbar}\int\limits_{r_2}^{r_3} \mathrm{d}r \sqrt{V(r) - Q}\,, \tag{5}$$

where Q is the energy released in cluster decay process and $V(r)$ is effective potential between daughter and cluster nucleus; r_i are turning points and μ reduced mass of the cluster–daughter system.

The effective potential includes attractive nuclear potential V_{N}, repulsive Coulomb potential V_{C}, and additional repulsive centrifugal part V_{cf}, and is given by

$$V(r) = \eta V_{\mathrm{N}}(r) + V_{\mathrm{C}}(r) + V_{\mathrm{cf}}(r)\,, \tag{6}$$

where η is a quantization factor. Based on double-folding method, the nuclear potential V_{N} is calculated as

$$V_{\mathrm{N}}(r) = \int \mathrm{d}\vec{r}_1 \mathrm{d}\vec{r}_2 \rho_{\mathrm{c}}(\vec{r}_1) v(s) \rho_{\mathrm{d}}(\vec{r}_2)\,, \tag{7}$$

where $s = |\vec{r}_2 - \vec{r}_1 + \vec{r}|$ is the relative distance between interacting nucleon pair. v is the nucleon–nucleon interaction potential. $\rho_\mathrm{c}(\vec{r}_1)$ and $\rho_\mathrm{d}(\vec{r}_2)$ are the matter density distributions of the cluster and daughter nucleus, respectively. The matter density distribution of the cluster (or daughter) is given via the two-parameter Fermi distribution as

$$\rho(r) = \frac{\rho_0}{1 + \exp\left[\frac{r - R_0}{a_0}\right]}\,, \tag{8}$$

where half-density radius is $R_0^{\mathrm{d(c)}} = 1.07 A_{\mathrm{d(c)}}^{1/3}$ [fm] and surface diffuseness parameter is $a_0 = 0.54$ [fm] [23]. The parameter $\rho_0^{\mathrm{d(c)}}$ is determined as $A_{\mathrm{d(c)}} = \int \mathrm{d}v \rho_{\mathrm{d(c)}}(r)$.

The effective nucleon–nucleon potential Yukawa (M3Y)-Paris-type interaction with zero-range exchange contribution is given as [21]

$$v(s) = 11062 \frac{e^{-4s}}{4s} - 2537 \frac{e^{-2.5s}}{2.5s} - 592(1 - 0.003 E_\mathrm{c}/A_\mathrm{c})\delta(s)\,, \tag{9}$$

where $E_\mathrm{c} = Q(A_\mathrm{d}/A_\mathrm{p})$. A_c, A_d and A_p are mass numbers of the cluster, daughter, and parent, respectively.

The Coulomb potential is calculated as

$$V_\mathrm{C}(r) = \begin{cases} \frac{1}{4\pi\varepsilon_0} \frac{Z_\mathrm{d} Z_\mathrm{c} e^2}{2R_\mathrm{C}} \left(3 - \frac{r^2}{R_\mathrm{C}^2}\right)\,, & r \le R_\mathrm{C}\,, \\ \frac{1}{4\pi\varepsilon_0} \frac{Z_\mathrm{d} Z_\mathrm{c} e^2}{r}\,, & r \ge R_\mathrm{C}\,. \end{cases} \tag{10}$$

The centrifugal potential is written as

$$V_\mathrm{cf}(r) = \frac{\hbar^2 l(l+1)}{2\mu r^2}\,, \tag{11}$$

where, by using Langer modification, we have $l(l+1) \to (l+1/2)^2$. μ is the reduced mass of the cluster–daughter system. l is the orbital angular momentum of the cluster nucleus. The values of l are determined according to the spin-parity selection rule

$$\begin{aligned} |J_\mathrm{p} - J_\mathrm{d}| &\le l \le J_\mathrm{p} + J_\mathrm{d}\,, \\ \frac{\pi_\mathrm{p}}{\pi_\mathrm{d}} &= (-1)^l\,, \end{aligned} \tag{12}$$

where J is spin and π is parity of parent (p) and daughter (d) nuclei.

The normalization factor η is determined by using the Bohr–Sommerfeld quantization condition for cluster decay [23]

$$\int\limits_{r_1}^{r_2} \mathrm{d}r \sqrt{\frac{2\mu}{\hbar^2}[Q - V(r)]} = (G_\mathrm{c} - l + 1)\frac{\pi}{2}\,, \tag{13}$$

where parameter G is the global quantum number determined by using the Wildermuth quantum rule. The global quantum number values for cluster nuclei are given as $G_{\rm c} = G_\alpha A_{\rm c}/4$ [17, 24], where G_α is given as [23]

$$G_\alpha = \begin{cases} 22 & N > 126 \\ 20 & 82 < N \leq 126\,. \\ 18 & N \leq 82 \end{cases}$$

The calculated double-folding nuclear potential of the system of ^{20}O cluster nuclei and ^{208}Pb daughter nuclei by inclusion of the quantization condition has been plotted in Fig. 1.

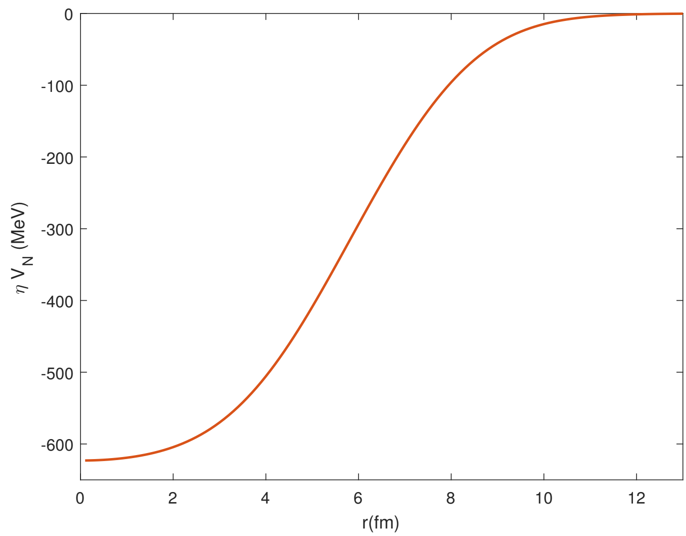

Fig. 1. Double-folding nuclear potential of ^{20}O cluster decay of ^{228}Th nuclei.

In order to evaluate the effect of the shape of the nuclear potential on cluster decay half-life, two phenomenological nuclear potentials, Woods–Saxon (WS) potential

$$V_{\rm N}(r) = \frac{V_0}{1+e^{\frac{r-R}{a}}}\,, \tag{14}$$

and cut-off Woods–Saxon (CWS) potential

$$V_{\rm N}(r) = \frac{V_0}{1+e^{\frac{r-R}{a}}}\ \delta\left(R_{\rm max}-r\right)\,, \tag{15}$$

were used. The $\delta(x)$ is the step function. Because of comparative analysis, the same values of the nuclear well depth $V_0 = -160$ MeV, interaction radius

$R = r_0(A_c^{1/3} + Ad^{1/3})$ with $r_0 = 1$ fm, surface diffuseness parameter $a = 0.54$ fm were adopted for both potentials. The position of cut-off potential was considered as $R_{max} = 1.15R \approx R_c + R_d$. In Fig. 2, we show the shapes of WS and CWS nuclear potentials for ^{20}O cluster and ^{208}Pb daughter nuclei.

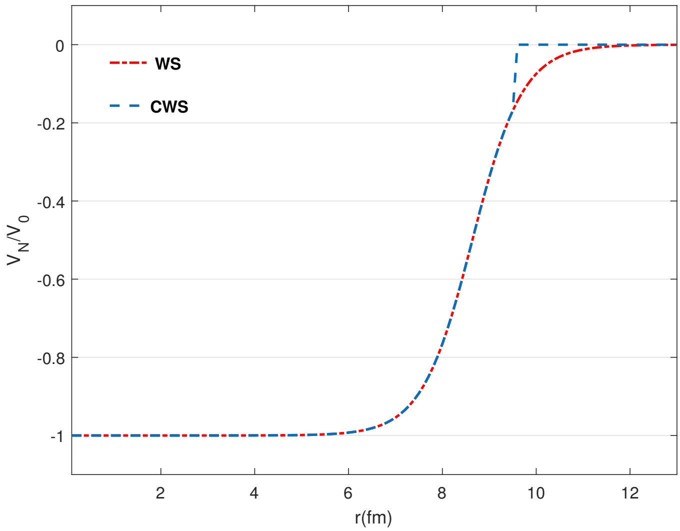

Fig. 2. WS and CWS nuclear potentials form factor for ^{20}O cluster decay of ^{228}Th nuclei.

Different empirical formulas have been introduced for cluster preformation probability [25–27]. We have used the following formula [27]:

$$\log S_c = a\sqrt{\mu Z_c Z_d} + b\,, \tag{16}$$

where $a = -0.052$, $b = 0.69$ for even–even nuclei and $b = -0.6$ for odd–A nuclei. Z_c and Z_d are atomic numbers of cluster and daughter nuclei, respectively.

The experimental cluster preformation probability, S_c^{exp}, inside the parent nucleus can be determined from the experimental half-life as

$$S_c^{exp} = \frac{T_{1/2}^{cal}}{T_{1/2}^{exp}}\,. \tag{17}$$

3. Results

The model described in the previous section is now applied to obtain the cluster decay half-lives of some heavy nuclei. The obtained results have been listed in Table I. The minimum angular momentum of cluster l_{min} has been determined by using total angular momentum and parity of parent and daughter. The total angular momentum has been adopted from nrv website [28]. The Q-value has been extracted from [29]. In columns 6–8, $\log T_{1/2}^{(\mathrm{I})}$, $\log T_{1/2}^{(\mathrm{II})}$, $\log T_{1/2}^{(\mathrm{III})}$, denote calculated cluster decay half-lives with double-folding, WS, and CWS potentials with including calculated cluster preformation probability $S_{\mathrm{c}}^{(\mathrm{I})}$. Columns 7 and 8 give experimental half-lives, $\log T_{1/2}^{(\mathrm{exp})}$, and corresponding references.

TABLE I

Cluster decay half-lives.

Cluster decay	l_{min}	Q [MeV]	$\log S_{\mathrm{c}}^{(\mathrm{I})}$	$\log S_{\mathrm{c}}^{\mathrm{I(exp)}}$	$\log T_{1/2}^{(\mathrm{I})}$	$\log T_{1/2}^{(\mathrm{II})}$	$\log T_{1/2}^{(\mathrm{III})}$	$\log T_{1/2}^{\mathrm{exp}}$	Ref.
^{221}Fr→^{14}C+^{207}Tl	3	31.29	−3.46	−3.40	$14.58^{+1.86}_{-1.58}$	12.63	13.67	$14.52^{+0.06}_{-0.05}$	[32]
^{221}Ra→^{14}C+^{207}Pb	3	32.40	−3.49	−3.39	$13.52^{+1.83}_{-1.61}$	11.52	12.57	$13.42^{+0.68}_{-0.25}$	[32]
^{222}Ra→^{14}C+^{208}Pb	0	33.05	−3.49	−2.27	$12.21^{+1.73}_{-1.71}$	10.20	11.25	$11.00^{+0.07}_{-0.06}$	[33]
^{223}Ra→^{14}C+^{209}Pb	4	31.84	−3.49	−4.83	$13.87^{+1.75}_{-1.71}$	12.15	13.36	$15.21^{+0.08}_{-0.07}$	[33]
^{224}Ra→^{14}C+^{210}Pb	0	30.54	−3.49	−3.31	$16.05^{+1.88}_{-1.62}$	14.41	15.60	$15.87^{+0.14}_{-0.11}$	[33]
^{226}Ra →^{14}C+^{212}Pb	0	28.20	−3.49	−3.56	$21.19^{+1.89}_{-1.64}$	19.40	20.55	$21.24^{+0.18}_{-0.13}$	[34]
^{226}Th→^{14}C+^{212}Po	0	30.55	−3.24	—	$16.14^{+1.72}_{-1.58}$	16.69	17.78	>15.30	[35]
^{226}Th→^{18}O+^{208}Pb	0	45.73	−4.73	—	$19.86^{+1.64}_{-2.87}$	16.03	17.29	>15.30	[35]
^{228}Th→^{20}O+^{208}Pb	0	44.73	−5.00	−2.95	$22.92^{+2.70}_{-1.87}$	18.80	20.17	$20.87^{+0.23}_{-0.15}$	[36]
^{230}Th→^{24}Ne+^{206}Hg	0	57.76	−6.13	−5.51	$25.25^{+2.60}_{-2.97}$	20.83	22.44	24.64	[36]
^{232}Th→^{26}Ne+^{206}Hg	0	55.97	−6.38	—	$29.47^{+2.34}_{-3.36}$	24.42	26.13	>29.20	[1]
^{231}Pa→^{23}F+^{208}Pb	1	51.86	−7.03	—	$25.63^{+2.78}_{-2.29}$	21.98	23.52	>24.61	[36]
^{231}Pa→^{24}Ne+^{207}Tl	1	60.42	−6.17	−6.08	$22.99^{+2.12}_{-3.33}$	18.13	19.75	$22.89^{+0.06}_{-0.05}$	[37]
^{230}U→^{22}Ne+^{208}Pb	0	61.40	−5.95	—	$21.16^{+2.89}_{-2.42}$	17.35	18.84	>18.20	[35]
^{230}U→^{24}Ne+^{206}Pb	0	61.36	−6.21	—	$23.04^{+2.25}_{-3.51}$	18.18	19.81	>18.20	[35]
^{232}U→^{24}Ne+^{208}Pb	0	62.31	−6.22	−6.14	$20.47^{+3.24}_{-2.18}$	16.77	18.40	$20.40^{+0.04}_{-0.03}$	[38]
^{232}U→^{28}Mg+^{204}Hg	0	74.33	−7.30	—	$25.52^{+2.83}_{-3.38}$	20.23	22.09	>22.65	[39]
^{233}U→^{24}Ne+^{209}Pb	2	60.51	−6.22	−8.82	$22.23^{+2.9}_{-2.58}$	18.66	20.56	$24.84^{+0.04}_{-0.04}$	[40]
^{233}U→^{25}Ne+^{208}Pb	2	60.75	−7.63	−6.45	$24.48^{+3.30}_{-2.26}$	20.74	22.40	23.30	[1]
^{233}U→^{28}Mg+^{205}Hg	3	74.25	−7.41	—	$28.63^{+4.33}_{-1.94}$	23.34	25.14	>27.59	[40]
^{234}U→^{24}Ne+^{210}Pb	0	58.84	−6.22	−6.72	$24.57^{+3.06}_{-2.24}$	21.03	22.88	$25.07^{+0.12}_{-0.65}$	[41]
^{234}U→^{26}Ne+^{208}Pb	0	59.47	−6.47	−6.13	$25.41^{+3.52}_{-2.18}$	20.43	23.33	$25.07^{+0.12}_{-0.65}$	[41]
^{234}U→^{28}Mg+^{206}Hg	0	74.13	−7.31	−7.47	$25.38^{+4.08}_{-2.15}$	23.34	22.28	$25.54^{+0.34}_{-0.34}$	[41]
^{235}U→^{24}Ne+^{211}Pb	1	57.36	−6.22	−5.56	$28.11^{+1.94}_{-3.58}$	24.65	25.15	$27.44^{+0.33}_{-0.19}$	[38]
^{235}U→^{25}Ne+^{210}Pb	3	57.73	−7.64	−5.64	$29.45^{+1.90}_{-3.77}$	26.08	26.55	$27.44^{+0.33}_{-0.19}$	[38]
^{235}U→^{28}Mg+^{207}Hg	1	72.21	−7.41	—	$31.63^{+3.23}_{-3.07}$	25.53	27.83	>28.45	[42]
^{236}U→^{24}Ne+^{212}Pb	0	55.96	−6.22	—	$29.21^{+3.16}_{-2.37}$	25.23	27.32	>26.28	[42]
^{236}U→^{26}Ne+^{210}Pb	0	56.75	−6.47	—	$30.09^{+2.04}_{-3.73}$	25.23	27.20	>26.28	[42]
^{236}U→^{30}Mg+^{206}Hg	0	72.48	−7.55	−7.90	$27.23^{+4.64}_{-1.81}$	23.22	25.17	27.58	[43]
^{237}Np→^{30}Mg+^{207}Tl	2	74.99	−7.61	—	$25.35^{+4.56}_{-1.92}$	21.20	23.16	>27.57	[44]
^{236}Pu→^{28}Mg+^{208}Pb	0	79.67	−7.41	−7.67	$21.41^{+3.08}_{-3.57}$	16.22	18.10	21.67	[45]
^{238}Pu→^{28}Mg+^{210}Pb	0	75.93	−7.42	−9.30	$23.79^{+4.16}_{-2.52}$	20.05	22.20	$25.69^{+0.25}_{-0.25}$	[46]
^{238}Pu→^{30}Mg+^{208}Pb	0	77.00	−7.66	−8.29	$25.04^{+3.60}_{-2.92}$	19.99	21.96	$25.69^{+0.25}_{-0.25}$	[46]
^{238}Pu→^{32}Si+^{206}Hg	0	91.21	−8.58	−5.06	$28.80^{+4.04}_{-3.03}$	22.88	24.92	$25.30^{+0.16}_{-0.16}$	[46]
^{240}Pu→^{34}Si+^{206}Hg	0	91.05	−8.71	—	$25.81^{+3.72}_{-3.49}$	20.22	22.44	>24.20	[1]
^{241}Am→^{34}Si+^{207}Tl	3	93.94	−8.77	—	$24.07^{+4.07}_{-3.67}$	18.36	20.59	>25.32	[47]

In order to evaluate the uncertainties of the calculated half-lives with double-folding potential, the uncertainties of the two parameters r_0 and a in nuclear matter density distribution of cluster and daughter nuclei in Eq. (8) were taken into account as $r_0 = 1.07 \pm 0.02$ [fm] and $a = 0.54 \pm 0.07$ [fm] [30].

Figure 3 displays the calculated half-lives, $\log T^{(\mathrm{I})}_{1/2}$, and experimental $\log T^{\mathrm{exp}}_{1/2}$ with corresponding errors. This figure have been depicted for cluster emitters ^{221}Fr(^{14}C), ^{221}Ra(^{14}C), ^{222}Ra(^{14}C), ^{223}Ra(^{14}C), ^{224}Ra(^{14}C), ^{226}Ra(^{14}C), ^{228}Th(^{20}O), ^{231}Pa(^{24}Ne), ^{232}U(^{24}Ne), ^{233}U(^{24}Ne), ^{234}U(^{24}Ne), ^{234}U(^{26}Ne), ^{234}U(^{28}Mg), ^{235}U(^{24}Ne), ^{235}U(^{25}Ne), ^{238}Pu(^{28}Mg), ^{238}Pu(^{30}Mg), ^{238}Pu(^{32}Si).

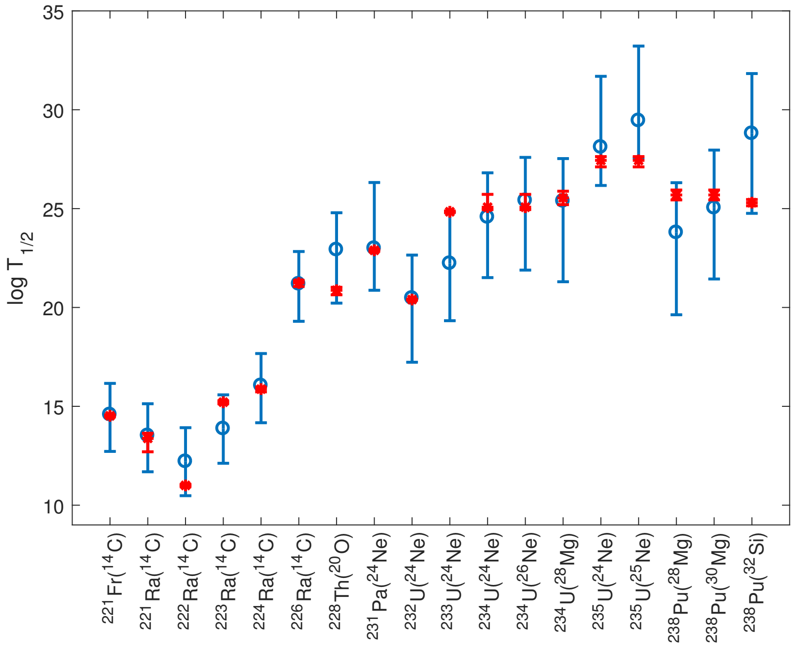

Fig. 3. Cluster decay half-lives. The circle and star denote $\log T^{(\mathrm{I})}_{1/2}$ and $\log T^{\mathrm{exp}}_{1/2}$, respectively.

The noticeable uncertainty in calculated half-lives with double-folding potential is observed. For heavier cluster emitters, the uncertainty is increased. These uncertainties show the sensitivity of double-folding calculations to the adopted values of r_0 and a parameters, especially the value of the surface diffuseness parameter. However, as investigated in our recent work [31], this sensitivity is anticipated.

As can be seen from Table I and Fig. 3, good agreement between calculated and experimental half-lives with double folding potential is observed. As expected, by the increase of weight of clusters, the cluster preformation probability is decreased, except cluster decays with double magic daughter nuclei.

The calculated half-lives with CWS potential are closer to the experiment in comparison with WS potential. Figure 4 displays the difference between calculated half-lives with WS and CWS potentials. As expected, larger half-lives are obtained with CWS. The difference is increased for heavier cluster emitters. This figure also shows noticeable role of cut-off distance ($R_{\max}$) in cluster decay calculations.

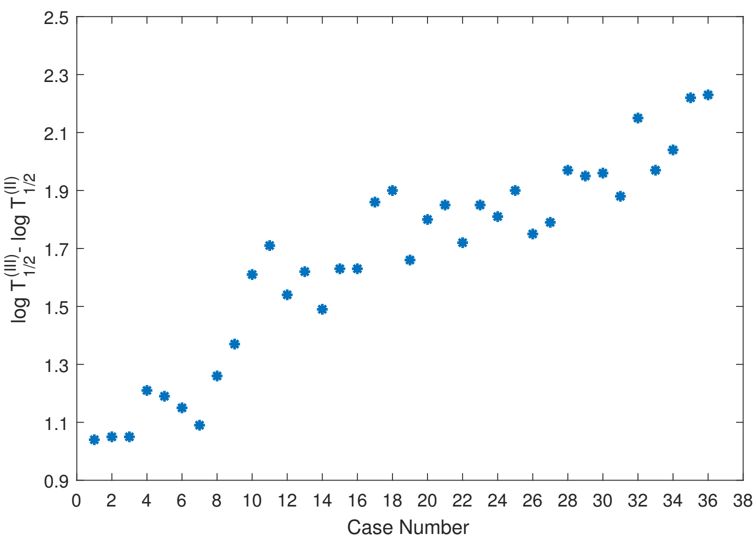

Fig. 4. Difference between calculated half-lives with WS and CWS.

By using the following relation, the standard deviation between logarithm of experiment and calculated half-lives can be determined

$$\sigma = \left[\frac{1}{n-1}\sum_{i=1}^{n}\left(\log T_{1/2}^{\mathrm{cal}} - \log T_{1/2}^{\mathrm{exp}}\right)^2\right]^{1/2} . \tag{18}$$

By considering the distinct values of experimental half-live of 18 cluster emitters, the standard deviation is obtained as $\sigma = 1.34$ for double-folding potential, $\sigma = 3.74$ for WS potential, and $\sigma = 2.32$ for CWS potential. It is worthwhile to note that calculated half-lives and, consequently, standard deviation are strictly dependent on the adopted values or formulas of the cluster preformation probability. These results show the effective role of cut-off in calculation of cluster decay half-lives. Comparison between calculated standard deviation based on double-folding potential, CWS potentials, and 14 types of proximity potentials in Ref. [18], with ranges from 1.373 up to 7.951, shows that double folding gives better results in all cases and CWS potential in 6 cases.

4. Discussion and conclusion

In this theoretical study, the cluster decay half-lives of 36 cluster emitters from ^{221}Fr to ^{241}Am with heavy clusters (heavier than alpha particle) were calculated by using double-folding potential. By considering the uncertainties of the radius and surface diffuseness in nuclear matter distribution, the uncertainties of calculated half-lives were determined. The obtained data were in good agreement with the experiment. Moreover, the sensitivity of calculations to the adopted valued of surface diffuseness were revealed. The noticeable role of the shape of the potential in calculations was detected by using phenomenological nuclear potentials WS and CWS.

REFERENCES

[1] G. Royer, R. Moustabchir, *Nucl. Phys. A* **683**, 182 (2001).
[2] D.N. Poenaru, R.A. Gherghescu, W. Greiner, *Phys. Rev. Lett.* **107**, 062503 (2011).
[3] D.N. Poenaru, R.A. Gherghescu, W. Greiner, *Phys. Rev. C* **85**, 034615 (2012).
[4] A. Bhagwat, R.J. Liotta, *Phys. Rev. C* **94**, 044312 (2015).
[5] Shicheng Wang *et al.*, *Phys. Rev. C* **36**, 2717(R) (1987).
[6] K.J. Moody, E.K. Hulet, Shicheng Wang, P.B. Price, *Phys. Rev. C* **39**, 2445 (1989).
[7] M. Hussonnois *et al.*, *Phys. Rev. C* **43**, 2599 (1991).
[8] R. Bonetti *et al.*, *Nucl. Phys. A* **556**, 115 (1993).
[9] R. Bonetti, A. Guglielmetti, *Rom. Rep. Phys.* **59**, 301 (2007).
[10] A. Sandulescu, D.N. Poenaru, W. Greiner, *Sov. J. Part. Nucl.* **11**, 528 (1980).
[11] H.J. Rose, G.A. Jones, *Nature* **307**, 245 (1984).
[12] D.S. Delion, A. Insolia, R.J. Liotta, *J. Phys. G* **19**, L189 (1993); **20**, 1483 (1994).
[13] D. Naderi, *Int. J. Mod. Phys. E* **22**, 1350065 (2013).
[14] A. Adel, T. Alharbi, *Nucl. Phys. A* **958**, 187 (2017).
[15] K.P. Santhosh, P. Priyanka, M.S. Unnikrishnan, *Nucl. Phys. A* **889**, 29 (2012).
[16] A. Soylu, Y. Sert, O. Bayrak, I. Boztosun, *Eur. Phys. J. A* **48**, 128 (2012).

[17] A. Soylu, S. Evlice, *Nucl. Phys. A* **936**, 59 (2015).
[18] G.L. Zhang *et al.*, *Nucl. Phys. A* **951**, 86 (2016).
[19] T.T. Ibrahima, S.M. Wyngaardtb, B.D.C. KimeneKaya, *Nucl. Phys. A* **966**, 73 (2017).
[20] A. Soylu, L.M. Robledo, M. Warda, *Int. J. Mod. Phys. E* **27**, 1850005 (2018).
[21] G.R. Satchler, W.G. Love, *Phys. Rep.* **55**, 183 (1979).
[22] S. Dahmardeh, S.A. Alavi, V. Dehghani, *Nucl. Phys. A* **963**, 68 (2017).
[23] C. Xu, Z. Ren, *Phys. Rev. C* **74**, 014304 (2006).
[24] B. Buck, A.C. Merchant, S.M. Perez, *Nucl. Phys. A* **657**, 267 (1999).
[25] R. Blendowske, H. Walliser, *Phys. Rev. Lett.* **61**, 1930 (1988).
[26] K. Wei, H.F. Zhang, *Phys. Rev. C* **96**, 021601(R) (2017).
[27] D. Ni, Z. Ren, *Phys. Rev. C* **82**, 024311 (2010); D. Ni, Z. Ren, T. Dong, C. Xu, *Phys. Rev. C* **78**, 044310 (2008).
[28] V.I. Zagrebaev *et al.*, NRV: Low Energy Nuclear Knowledge Base, `http://nrv.jinr.ru/nrv`
[29] G. Audi, O. Bersillon, J. Blachot, A.H. Wapstra, *Nucl. Phys. A* **624**, 1 (1997).
[30] B. Hahn, D.G. Ravenhall, R. Hofstadter, *Phys. Rev.* **101**, 1131 (1956).
[31] V. Dehghani, S.A. Alavi, Kh. Benam, *Mod. Phys. Lett. A* **33**, 1850080 (2018).
[32] R. Bonetti *et al.*, *Nucl. Phys. A* **576**, 21 (1994).
[33] P.B. Price, J.D. Stevenson, S.W. Barwick, H.L. Ravn, *Phys. Rev. Lett.* **54**, 297 (1985).
[34] S.W. Barwick *et al.*, *Phys. Rev. C* **34**, 362(R) (1986).
[35] M. Hussonnois *et al.*, *Phys. Rev. C* **43**, 2599 (1991).
[36] R.K. Gupta, W. Greiner, *Int. J. Mod. Phys. E* **3**, 335 (1994).
[37] P.B. Price *et al.*, *Phys. Rev. C* **46**, 1939 (1992).
[38] R. Bonetti *et al.*, *Phys. Rev. C* **44**, 888 (1991).
[39] R. Bonetti *et al.*, *Phys. Lett. B* **241**, 179 (1990).
[40] P.B. Price *et al.*, *Phys. Rev. C* **43**, 1781 (1991).
[41] Shicheng Wang *et al.*, *Phys. Rev. C* **36**, 2717(R) (1987).
[42] S.P. Tretyakova *et al.*, *Z. Physik A* **333**, 349 (1989).
[43] S.P. Tretyakova *et al.*, *JETP Lett.* **59**, 394 (1994).
[44] K.J. Moody, E.K. Hulet, P.B. Price, *Phys. Rev. C* **45**, 1392 (1992).
[45] A.A. Oglobin *et al.*, *Phys. Lett. B* **235**, 35 (1990).
[46] Shicheng Wang *et al.*, *Phys. Rev. C* **39**, 1647(R) (1989).
[47] K.J. Moody *et al.*, *Phys. Rev. C* **36**, 2710(R) (1987).